Supporting Information

Two-phase dual-signal readout immunosensing platform based on multifunctional carbon nano-onions for ovarian cancer biomarker detection

Yitian Huang[a#], Shupei Zhang[b#], Yanjie Chen[a], Lihong Gao[b*], Hong Dai[b *], Yanyu Lin[a]

a College of Chemistry and Material, Fujian Normal University, Fuzhou, Fujian 350108, China

b College of Chemical and Material Engineering, Quzhou University, Quzhou, Zhejiang 324000, China

Corresponding author: Fax: (+86)-591-22866135; E-mail: luckydai666@163.com (H. Dai); lihonggao2023@21cn.com (L.H Gao) # Yitian Huang and Shupei Zhang contributed to the work equally and should be regarded as co-first authors.

TABLE OF CONTENTS

1. Experimental section

1.1. Materials and reagents

Ethanol ($CH_3CH_2OH \geq 99.7$ wt %) was purchased from Shanghai Titan Scientific Co. Ltd. Si-NH_2 magnetic bead (MB) was acquired from PuriMag Biotech Co. (Xiamen, China). Bovine serum albumin (BSA, 1 wt %) and Glutaraldehtyde (GLD, 25 wt % aqueous solution) were obtained from Biss Inc. (Beijing, China) and Jinshan Tingxin Chemical Plant (Shanghai, China), respectively. 1- aminoethyl-3-methylimidazolium chloride (Ionic liquid, ILs) was got by Lanzhou Institute of Chemical Physics, Chinese Academy of Sciences. Dimethyl sulfoxide (DMSO) was purchased from Sinopharm. Antibody (Ab) of human epididymis protein 4 (HE4) were produced by Wuhan San Ying Biotechnology Co., Ltd (China). HPV16 (E6) protein, human interleukin-6 (IL-6) and lipolysis stimulated lipoprotein receptor (LSR) were gained from Beijing biosen Biotechnology Co., Ltd. (China), Shanghai Linc-Bio Science Co. Ltd. (China) and Shanghai Genechem Co., LTD, respectively. The phosphate buffer solution (PBS, 0.1 M) of various pH was prepared by mixing the stock solution of 0.1 M Na_2HPO_4 and NaH_2PO_4. Aluminum titanium carbide (Ti_3AlC_2) was obtained from Forsman Technology Co., Ltd. (Beijing, China).

1.2. Apparatus

The SCL emission was generated on a mini USB ultrasonic atomizer that obtained from Shenzhen Jingdongshun Electronics Co. Ltd and measured on a chemiluminescence detector (Xi'an Remax Analysis Instrument Co., Xi'an, China). The solution temperature was adjusted by the 808 nm NIR light system. The ultra-

violet–visible absorption was measured on UV 1900 (Shanghai, Lengguang Tech). Fluorescence spectrum was conducted on F-380 spectrophotometer originated from Tianjin Gangdong Sci. &Tech. Co., Ltd. Transmission electron microscopy (TEM, FEI F20 S-TWIN instrument) was used to characterize the morphology of the materials. The temperature was monitored with a TES-1310 digital thermometer (TES electrical electronic corp. Taiwan, China)

2. Supplementary experimental data

Scheme S1

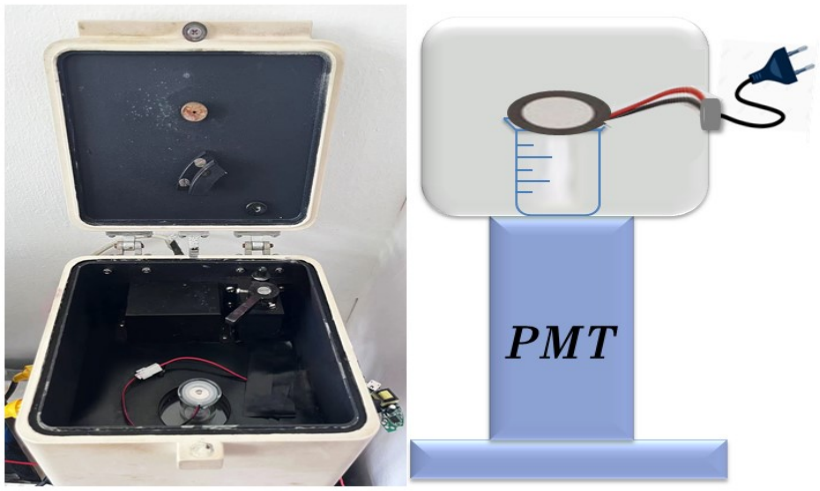

Scheme S1. Layout of the SCL signal acquisition.

Figure S1

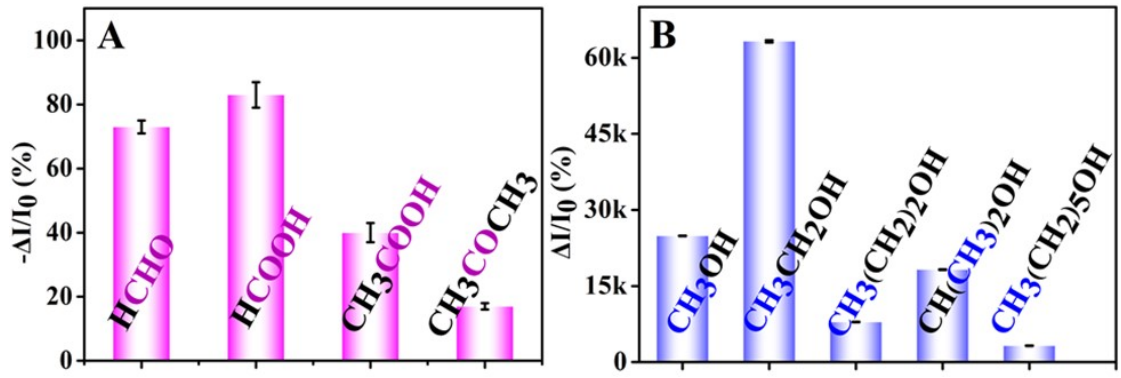

Figure S1. Influence of on SCL signal intensity in the presence of (A) organics with different groups and (B) alcohols with different numbers of methyl groups in Luc^{2+} /Ti_3C_2 NDs system.

Figure S2

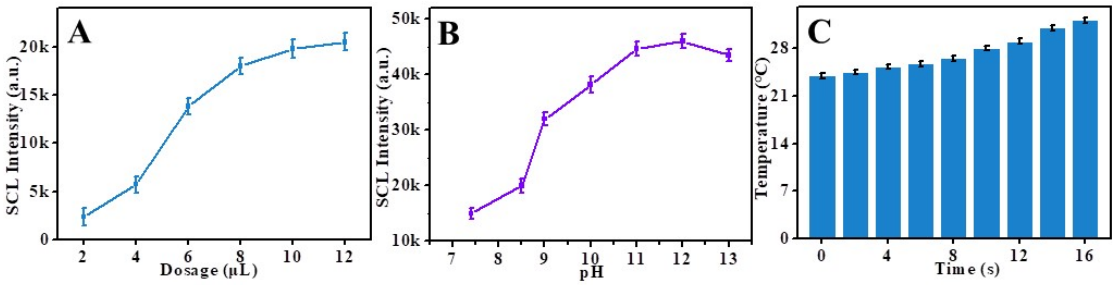

Figure S2. The effect of (A) dosage of Ti_3C_2 NDs and (B) pH on the SCL intensity of Luc^{2+}/ethanol/Ti_3C_2 NDs system. (C) The variation of temperature of the Luc^{2+}/ethanol/Ti_3C_2 NDs system with ultrasonic time.

77 **Figure S3**

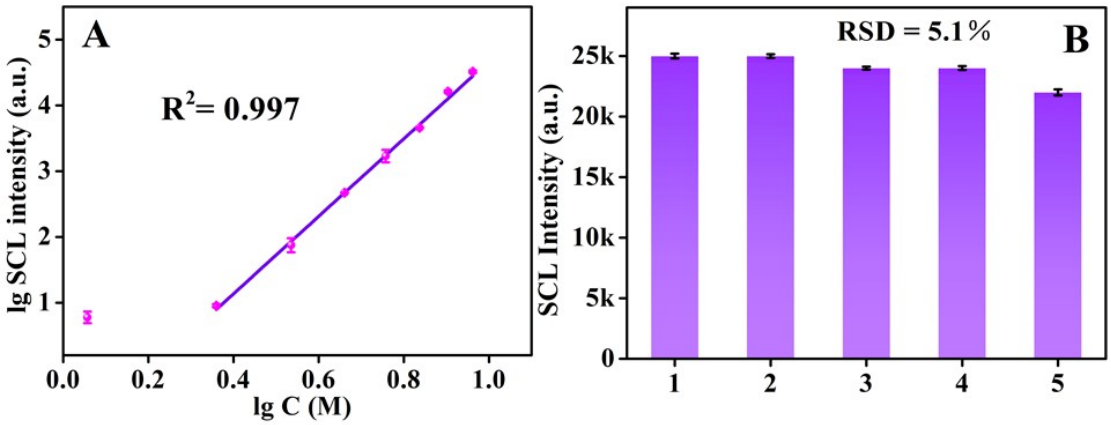

78

79 **Figure S3.** (A) SCL signals of the Luc^{2+}/Ti_3C_2 NDs with different concentrations of

80 ethanol in Luc^{2+}/Ti_3C_2 NDs system. (B) Reproducibility tests of five ultrasonic

81 atomizer with 8 M ethanol in the Luc^{2+}/Ti_3C_2 NDs system.

82

Figure S4

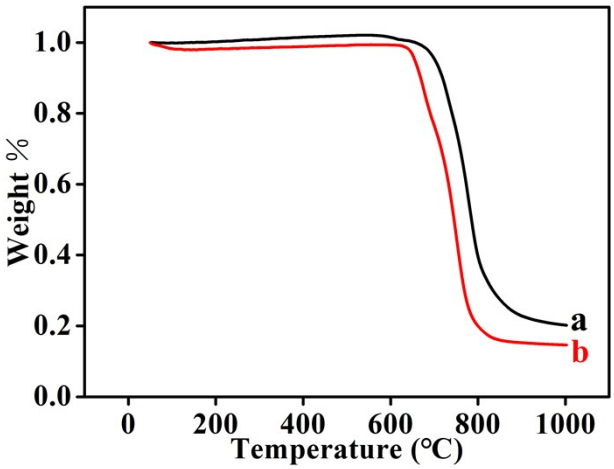

Figure S4. Thermogravimetric analysis curves of (a) pure CNOs, (b) CNOs with adsorbed ethanol.

Figure S5

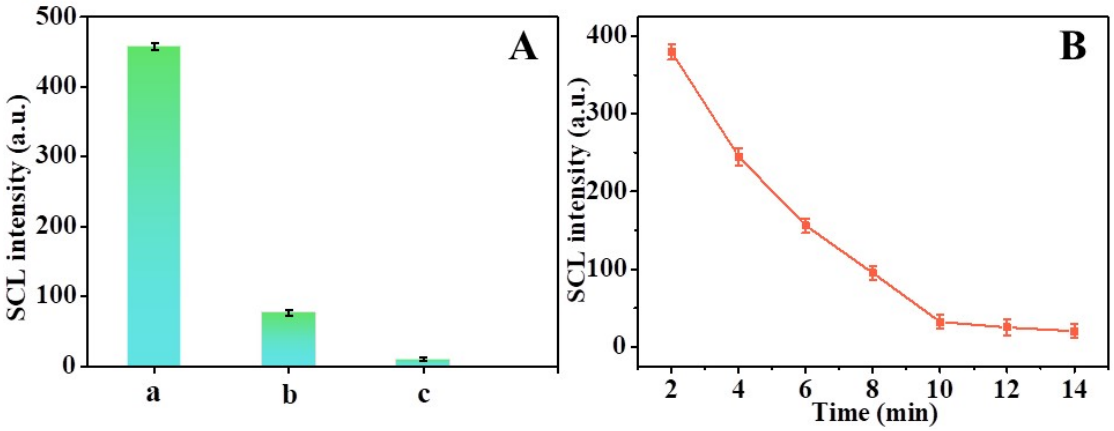

Figure S5. (A) SCL intensity of the Luc^{2+}/Ti_3C_2 NDs system with the remaining ethanol after adsorption of different materials (a) blank, (b) carbon nanohorns and (c) CNOs. (B) Optimization of ethanol adsorption time by CNOs.

Figure S6

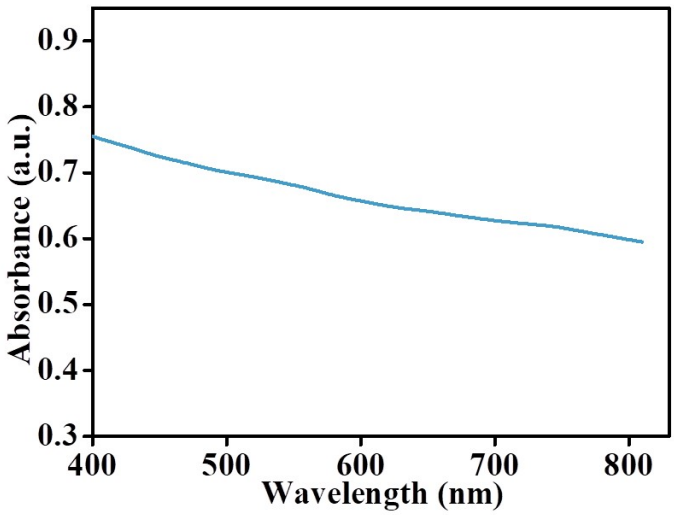

Figure S6. UV−vis spectrum of CNOs.

Figure S7

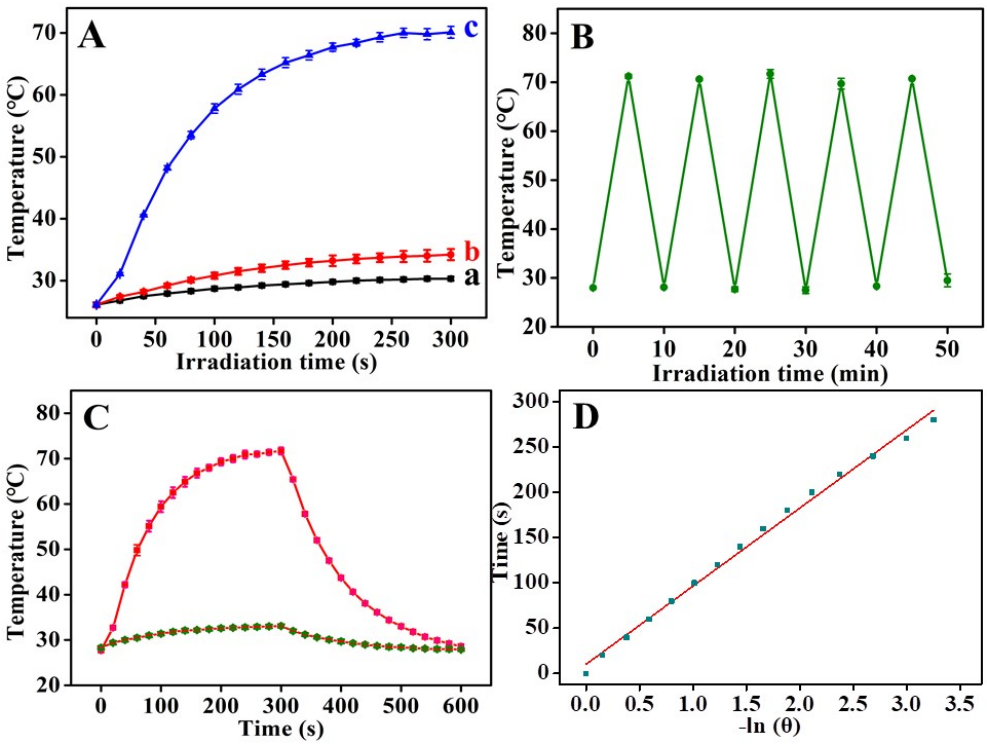

Figure S7. (A) Temperature variation of the different materials under 300 s of 808 nm laser irradiation with a power density of 1 W·cm^{-2} (a) water (b) Si-NH_2 MB (0.1 mg/mL), and (c) CNOs (0.75 mg/mL). (B) Photothermal stability of CNOs. (C) Photothermal effect of H_2O (green line) and CNOs (red line) under 808 nm laser (1 W·cm^{-2}) for 5 min, followed by natural cooling as the laser turns off. (D) The time-(-lnθ) plot for applying the linear slope of the cooling period to calculate hA.

The photothermal performance of CNOs as a temperature signal output was explored. As displayed in Fig. S7A, the temperature of water (curve a) and Si-NH_2 MB (curve b) had no obvious fluctuation under irradiation with 1 W·cm^{-2} power density of 808 nm laser for five minutes. However, the temperature of 0.75 mg/mL CNOs dispersion (curve c) significantly increased from 26.1 ℃ to 70.1 ℃ under radiation of the laser. Moreover, the photothermal stability of CNOs was investigated upon five laser on/off cycles as exhibited in Fig. S7B, and there was no significant

112 difference in the temperature change during the five cycles. This proved that CNOs
113 have good photothermal stability. More importantly, the photothermal conversion
114 efficiency (η) of CNOs was also calculated according to the following equation：

$$\eta = \frac{hA(\Delta T_{max} - \Delta T_0)}{I(1-10^{-A'_\lambda})}$$

$$\theta = \frac{\Delta T_i}{\Delta T_{max}}$$

115

$$hA = \frac{mc}{slope\ of\ time\ -\ \left[-ln(\theta)\right]}$$

116 where ΔT_0 and ΔT_{max} are the maximum increase temperature of solvent (4.3 ℃ for
117 water) and photothermal materials (44 ℃ for CNOs), ΔT_i is the increase in
118 temperature measured at any time, m is mass of solution (0.1g), c is heat capacity of
119 solution (4.2 $J \cdot g^{-1}$), I is laser power density (1 $W \cdot cm^{-2}$), and A'_λ is the absorbance of
120 the CNOs solution at 808 nm (1.597).

121

Figure S8

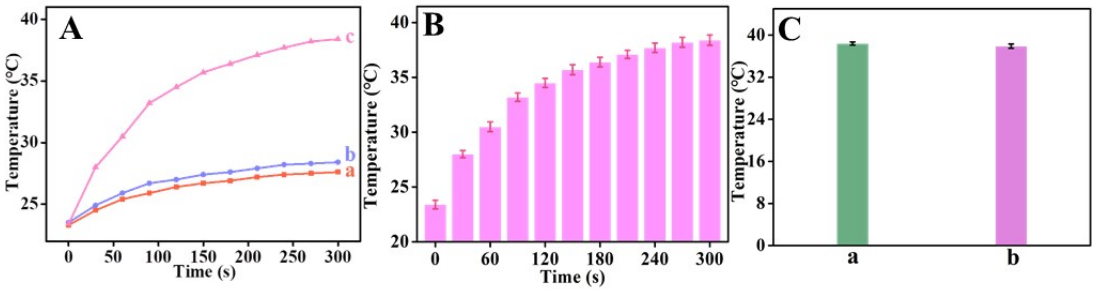

Figure S8. (A) Effect of temperature variation of different probes on the immune construct process. (a) HE4, (b) CNOs and (c) CNOs@HE4. (B) The optimization of 808 nm laser irradiation time. (C) Temperature signal of (a) PBS/CNOs@HE4/BSA/Ab/GLD/MB and (b) ethanol/CNOs@HE4 /BSA/Ab/GLD/MB after magnetic separation.

131 **Figure S9**

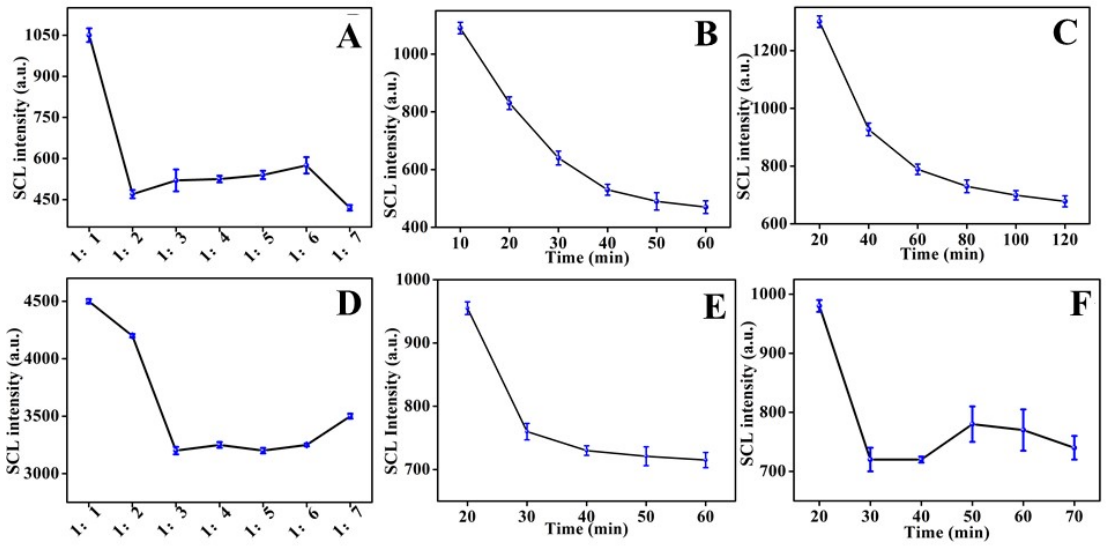

132

133 **Figure S9.** The optimization of (A) the ratio of CNOs to HE4, (B) the connection
134 time between CNOs and HE4, (C) the time to immobilize Ab with MB, (D) the ratio
135 of MB to Ab, (E) the competitive time, and (F) CNOs adsorption time for ethanol.

136

Table S1

Comparisons of the constructed two-phase signal reading immunosensing platform with other methods for HE4.

Method	Linear range (ng mL^{-1})	Detection limit (ng mL^{-1})	Reference
Photoelectrochemical immunoassay	0.01 ~ 200	1.56×10^{-3}	[1]
chemiluminescence immunoassay	0.25 ~ 50	0.084	[2]
Electrochemical assay	1 ~ 100	0.2	[3]
Fluorescence method	1.25~20	0.16	[4]
SCL biosensor	10^{-5} ~ 1	3.3×10^{-6}	This work
Temperature readout	10^{-5} ~ 10	3.3×10^{-6}	

Table S2

Recoveries of the constructed two-phase signal reading immunosensing platform for detection of HE4 in human serum sample (n=3)[a].

Sample (ng/mL)	Added (ng/mL)	SCL found (ng/mL)	Recovery (%)	Temperature found (ng/mL)	Recovery (%)
1	10^{-1}	0.1039	103.9	0.0975	97.5
2	10^{-2}	1.01×10^{-2}	101	9.23×10^{-3}	92.3
3	10^{-3}	1.091×10^{-3}	109.1	1.107×10^{-3}	110.7
4	10^{-4}	0.9534×10^{-4}	95.34	1.049×10^{-4}	104.9

[a] n is the repetitive measurements number.

Recovery = $(C_{found}/C_{added}) \times 100\%$.

Reference

(1) Zhang, B.; Wang, H.; Xi, J.; Zhao, F.; Zeng, B., *Electrochimica Acta* **2020**, *331*.
(2) Zhao, H.; Lin, Q.; Huang, L.; Zhai, Y.; Liu, Y.; Deng, Y.; Su, E.; He, N., *Nanoscale* **2021**, *13*, 3275-3284.
(3) Qiao, Z.; Zhang, H.; Zhou, Y.; Zheng, J., *Anal Chem* **2019**, *91*, 5125-5132.
(4) Yao, S.; Xiao, W.; Chen, H.; Tang, Y.; Song, Q.; Zheng, Q.; Deng, N., *Analytical Methods* **2019**, *11*, 4814-4821.